Colloids and Surfaces B: Biointerfaces 107 (2013) 59–67

Contents lists available at SciVerse ScienceDirect

Colloids and Surfaces B: Biointerfaces

journal homepage: www.elsevier.com/locate/colsurfb

Controlled lateral packing of insulin monolayers influences neuron polarization in solid-supported cultures

E.J. Grasso, R.G. Oliveira, M. Oksdath, S. Quiroga, B. Maggio*

CIQUIBIC, UNC–CONICET, Departamento de Química Biológica, Facultad de Ciencias Químicas, Universidad Nacional de Córdoba, Haya de la Torre y Medina Allende, Ciudad Universitaria, X5000HUA, Córdoba, Argentina

ARTICLE INFO

Article history:
Received 17 December 2012
Received in revised form 24 January 2013
Accepted 29 January 2013
Available online xxx

Keywords:
Insulin Langmuir monolayer
Neuron polarization
Self-organized insulin films
Neuron surface recognition

ABSTRACT

Neurons are highly polarized cells, composed of one axon and several branching dendrites. One important issue in neurobiology is to understand the molecular factors that determine the neuron to develop polarized structures. A particularly early event, in neurons still lacking a discernible axon, is the segregation of IGF-1 (Insulin like Growth Factor-1) receptors in one neurite. This receptor can be activated by insulin in bulk, but, it is not known if changes of insulin organization as a monomolecular film may affect neuron polarization. To this end, in this work we developed solid-supported Langmuir–Blodgett films of insulin with different surface packing density. Hyppocampal pyramidal neurons, in early stage of differentiation, were cultured onto those substrates and polarization was studied after 24 h by confocal microscopy. Also we used surface reflection interference contrast microscopy and confocal microscopy to study attachment patterns and morphology of growth cones. We observed that insulin films packed at 14 mN/m induced polarization in a similar manner to high insulin concentration in bulk, but insulin packed at 44 mN/m did not induce polarization. Our results provide novel evidence that the neuron polarization through IGF-1 receptor activation can be selectively modulated by the lateral packing of insulin organized as a monomolecular surface for cell growth.

1. Introduction

A typical polarized neuron is composed of a single long axon and several branching dendrites. The initial signals and pathways that determine polarity are beginning to be understood. A large number of studies have been made on neuronal polarization that were focused on the actin cytoskeleton and its modulators such as Rho, Cdc42, profiling, cofilin and T-lymphoma and metastasis 1 protein [1–4]. Regarding regulation of neuron polarization by external factors, a particularly early event in neurons that do not yet exhibit a discernible axon, is the segregation of IGF-1 (Insulin like Growth Factor-1) receptors in one neurite [5]. IGF-1 exerts most of its biological actions through binding and activation of a specific membrane-associated tetrameric receptor containing an intracellular domain with tyrosine kinase activity [6]. This is followed by activation of the PIP3K pathway [12–14] which is critical for the outgrowth and elongation of the future axon [7], with addition of new membrane mainly at the neuronal growth cone [8–11].

For practical purposes, neuron polarization is frequently induced by insulin that also causes cell differentiation through binding to the IGF-1 receptor when added to bulk culture medium in relatively high concentrations [5,8]. On the other hand, insulin Langmuir monolayers at the air–water interface were previously studied under different experimental conditions such as pH, temperature and different ion concentration in the subphase; it has also been shown that the presence of zinc ions in the subphase has a profound effect on the surface behavior of the insulin monolayer [24–26]. This is a suitable system to study the influence of a defined and known lateral molecular organization of insulin on its ability to trigger a cellular response.

Several studies have shown that cellular response, in terms of recognition, adhesion, proliferation and differentiation, can be very sensitive to the molecular organization of the substrate onto which cells are grown [15–18]. Films of axolemma monolayers coated onto glass coverslips at defined surface molecular packing affected the Schwann cell morphology, their proliferative response, expression and subcellular distribution of specific membrane antigens [19,20]. Regarding neuronal cells, some studies have shown that extracellular substrate molecules can determine which neurite becomes an axon depending on the substrate preference for neurite elongation [21–23].

Thus, the purpose of our work was to assess possible differential responses of neuronal polarization induced by insulin when it is organized as a monomolecular layer under precisely controlled different molecular packing conditions as compared to its effects when added in bulk. The paper is divided in two major parts:

* Corresponding author. Tel.: +54 0351 5353855; fax: +54 0351 4334074.
E-mail addresses: bmaggio@fcq.unc.edu.ar, ejgrasso@conicet.gov.ar (B. Maggio).

0927-7765/$ – see front matter © 2013 Elsevier B.V. All rights reserved.
http://dx.doi.org/10.1016/j.colsurfb.2013.01.059

the first one refers to the construction and characterization of solid-supported insulin monolayers and the second describes the neuronal response to the substrate surface organization.

2. Materials and methods

2.1. Reagents

Bovine insulin (MW 5733 Da), octadecyltrichlorosilane and poly L-lysine (MW 30–70 kDa) were purchased from Sigma–Aldrich, St. Louis, MO, USA. Aqueous subphases were prepared with ultrapure water (resistivity 18.2 MΩ cm) produced by a Millipore water purification system. NaCl and $ZnCl_2$ were purchased from Merck (Darmstadt – Germany). Glass coverslips (12 mm diameter) was purchased from Marienfeld GmbH & Co. Kg, Germany. Culture mediums for neurons (Neurobasal and DMEM), including N2 mixtures, were purchased from Invitrogen, Carlsbad CA, USA.

2.2. Insulin monolayers

Langmuir monolayers of insulin were formed by spreading 10 μL of insulin solution (2.22 mg/mL) onto the aqueous surface (NaCl 145 mM or NaCl 145 mM plus $ZnCl_2$ 1 mM). Compression and decompression isotherms and surface potential measurements were carried out in a KSV-minitrough with a KSV capacitor like system (KSV Instruments Ltd., Helsinki, Finland), having a teflon trough with a surface area of 266 cm^2 and a Pt-Wilhelmy plate surface pressure sensor and two symmetrically moving barriers, enclosed in an acrylic box surrounded by a metallic grid connected to ground. Films were compressed at a speed of 10 mm/min. The temperature was maintained at 24 ± 0.5 °C with an external circulating water bath (Haake F3C). The collapse pressures, surface pressure points for insulin reorganization and limiting mean molecular areas of the insulin films were determined from the third derivative of the compression isotherms [27].

The surface compressional modulus (in-plane elasticity, C_s^{-1}) [28] was calculated directly from the surface pressure–mean molecular isotherm according to

$$C_s^{-1} = -A\left(\frac{\partial \pi}{\partial A}\right)$$

where A is the mean molecular area (MMA) and π is the surface pressure.

The resultant perpendicular dipole moment of insulin is directly proportional to the surface (dipole) potential per unit of molecular surface density ($\Delta V/n$) where n is the density of overall dipoles in the film (the inverse of the mean molecular area, MMA) at a defined surface pressure [28].

For film imaging, Brewster angle microscopy (BAM) was performed with an autonulling imaging ellipsometer (Nanofilm EP3sw imaging ellipsometer, Accurion Gmbh, Germany) equipped with a 532 nm laser, 10× and 20× objective, and a CCD camera. By using p-polarized light, the equipment automatically finds the actual Brewster angle of the subphase by measuring the intensity of reflected light at several angles of incidence and performs a calibration of the reflected light and the gray level intensity measured by the CCD camera.

2.3. Supported insulin monolayers

The insulin monolayers were coated onto alkyl-silanized or poly L-lysine-coated glass coverslips with a method employed previously [29]. Coverslips, first alkylated with octadecylthreechlorosilane, were held horizontally above the monolayer set at the desired surface pressure and automatically lowered at constant speed (0.25 cm/min) until they gently touched the monolayer surface. The coverslip was left to rest for 15 s over the surface, at constant surface pressure, and then pushed vertically through the monolayer at a speed synchronized with the servo-barostat in order to keep constant the surface pressure during coating. The coated coverslips were always handled under aqueous solutions to avoid collapse of the monolayer.

In another procedure, poly L-lysine-coated coverslips [30] were submerged vertically into the aqueous subphase prior to spreading the insulin monolayer. After formation of the film the coverslips submerged in the subphase solution were lifted up at a constant speed (1 mm/min) synchronized with the servo-barostat in order to keep constant the surface pressure during coating. Finally, these substrates were stored at room temperature in an exsiccator for 24 h for drying.

2.4. Cell culture

Dissociated hippocampal pyramidal neurons were prepared from fetal rat brain and cultured as described previously [30]. In summary, cell were plated onto insulin coated coverslips and maintained in DMEM plus 10% horse serum for 1 h. The coverslips with the attached cells were subsequently transferred to 35 mm Petri dishes containing Neurobasal and insulin-free medium plus the N2 mixture (except for some control cultures in which the insulin was added in the bulk medium the only insulin source comes from the coated coverslips). Cultures were maintained for 22–24 h in a humidified 37° C incubator with 5% CO_2.

2.5. Immunostaining, confocal and phase microscopy and surface reflective interference contrast

Cells were fixed for 20 min at room temperature with 4% (w/v) paraformaldehyde in PBS containing 4% (w/v) sucrose. Cultures were washed with PBS, permeabilized with 0.2% (v/v) Triton X-100 in PBS for 6 min, and again washed with PBS. After labeling with a primary antibody (β-III Tub, 1:4000, Calbiochem, and/or rhodamine-phalloidin, Sigma Co, 1:500, 1–3 h at room temperature) and washing with PBS, cultures were incubated with fluorescent secondary antibody (conjugated to Alexa Fluor 488, 1 h at 37°) and washed with PBS. Confocal images were collected using a Carl Zeiss LSM5 Pascal laser scanning confocal microscope (Carl Zeiss AG, Germany). Epifluorescence and phase contrast were viewed using a Zeiss Axioplan fluorescence microscopy (Carl Zeiss, Germany). For some experiments, cells were observed with a Nikon Eclipse TIRF with surface reflective interference contrast capacity microscope. SRIC images were captured using a CCD camera (Hamamatsu) and digitized directly into a MetaMorph/Metafluor Image Processor (Universal Imaging).

3. Results and discussion

3.1. Surface behavior of insulin monolayers

The surface pressure and surface potential-area isotherms and compression moduli of the insulin monolayer are shown in Fig. 1. The lift-off of the surface pressure corresponds to a sectional mean molecular area (MMA) of ~750 $Å^2$ $molecule^{-1}$, either for insulin spread onto NaCl 145 mM subphase or insulin spread onto NaCl 145 mM plus $ZnCl_2$ 1 mM subphase, in agreement with previous reports [31]. On decreasing the MMA from 750 to about 450 $Å^2$ a highly liquid expanded state of both insulin films convert to less liquid expanded. From a MMA of about 430 $Å^2$ (14 mN/m) the NaCl–insulin monolayer begins the transition to the collapsed state at about 22 mN/m. However, the $ZnCl_2$–insulin monolayer undergoes a surface pressure-induced reorganization whereupon

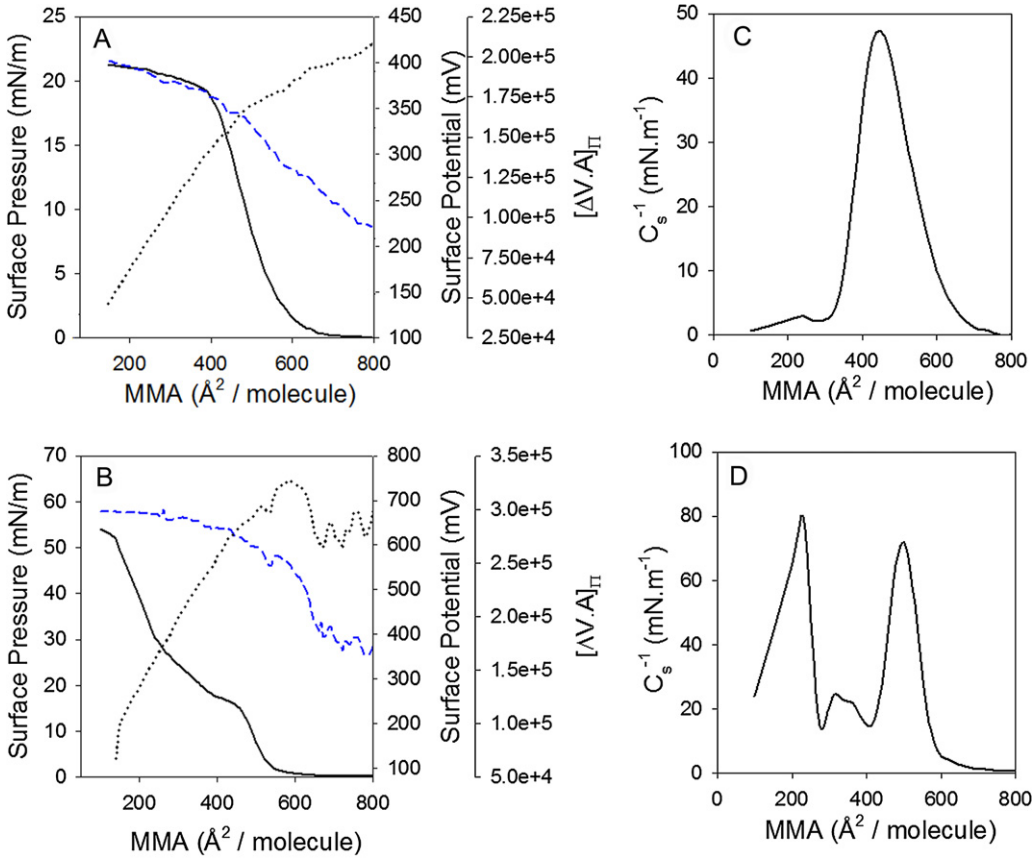

Fig. 1. Surface behavior of insulin Langmuir monolayers. (A) Surface pressure (continuous line), surface potential (dashed line) and surface potential per unit of molecular surface density ([$\Delta V \times A$], dotted line), as a function of the mean molecular area (MMA), for NaCl-insulin monolayer or $ZnCl_2$–insulin monolayer (B). (C) and (D) surface compressional moduli as a function of the MMA for the insulin monolayers shown in (A) and (B), respectively.

the film becomes more condensed between MMA of about 480 Å^2 (14 mN/m) and 390 Å^2 (18 mN/m). The collapse surface pressure for the $ZnCl_2$–insulin film occurred at ~50 mN/m. Such subphase(ion)-dependent behavior of insulin monolayers was previously reported by Nieto-Suárez et al. [24]. As observed in Fig. 1, the presence of Zinc ions in the subphase considerably increases the slope of the isotherm in the pre- and post-transition regions and shows a sharp slope change evidencing collapse at a MMA of about 150 Å^2 at ~50 mN/m. The slope changes of the isotherms were well reflected by the surface compressional modulus (C_s^{-1}) (Fig. 1C and D). On the other hand, the presence of Zinc ions in the subphase caused marked variations of the surface electrostatics of insulin monolayers. The higher surface potential reached at close packing by the $ZnCl_2$–insulin monolayer correlates with the more condensed reorganization. The variation with molecular packing of the surface potential per unit of molecular surface density ($\Delta V/n = \Delta V \times \text{MMA})_\pi$ is well correlated to the slope changes of the compression isotherms. The slope changes of ($\Delta V \times$ MMA) at 430 Å^2 (14 mN/m) for NaCl–insulin monolayer also coincides with the transition from a liquid-expanded to a more condensed state until collapse. The condensed-like behavior of $ZnCl_2$–insulin films was apparent in films observed by Brewster angle microscopy. As shown in Fig. 2A, immediately after spreading we observed patches in the monolayer that moved within a gaseous-like phase and an image of the liquid expanded monolayer could only be captured when the film acquired a coherent state after lift-off (above 1 mN/m). The high reflectivity (Fig. 2B) observed in $ZnCl_2$–insulin monolayer was concomitant with the behavior observed previously in the compression isotherms. It was proposed that the more condensed behavior of insulin on the subphase containing zinc ions is because the latter induce the formation of insulin hexamers [32]. Evidence suggesting formation of insulin hexamers at the air–water interface was provided by the work of Liu et al. [26] in which the presence of hexamers was inferred by Fourier transform infrared (FTIR) and polarization-modulated infrared reflection–absorption spectroscopy (PM-IRRAS) using human insulin monolayers. It was also deduced that an α-helix conformation was mostly maintained in the monolayer [26,31] and formation of hexamers could occur by an increase of β-strand structures due to aggregation [26]. However, in the absence of zinc the insulin monolayer was not aggregated and had an α-helix conformation over the whole isotherm [31].

3.2. *Neuron polarization modulated by the surface organization of insulin films transferred to poly L-lysine-coated coverslips*

It was ensured that the Langmuir–Blodgett transference of insulin films to treated coverslips was essentially complete (see supplementary material). The growth pattern of neurons cultured onto insulin monolayers transferred to alkyl-silanized coverslips was similar to that of cells grown onto insulin monolayers transferred to poly L-lysine coated coverslips but the cell attachment to the latter was higher (data not shown). Thus, as a routine, we used insulin monolayers transferred onto poly L-lysine coated coverslips as a substrate to plate hippocampal neurons. Fig. 3 shows neurons cultured onto $ZnCl_2$–insulin monolayers packed at 14 and 44 mN/m (Fig. 3A and C, respectively). As controls we co-cultured neurons grown onto poly L-lysine coated coverslips without insulin films (Fig. 3B and D, respectively). It is important to emphasize that controls correspond to neurons grown onto poly L-lysine coated

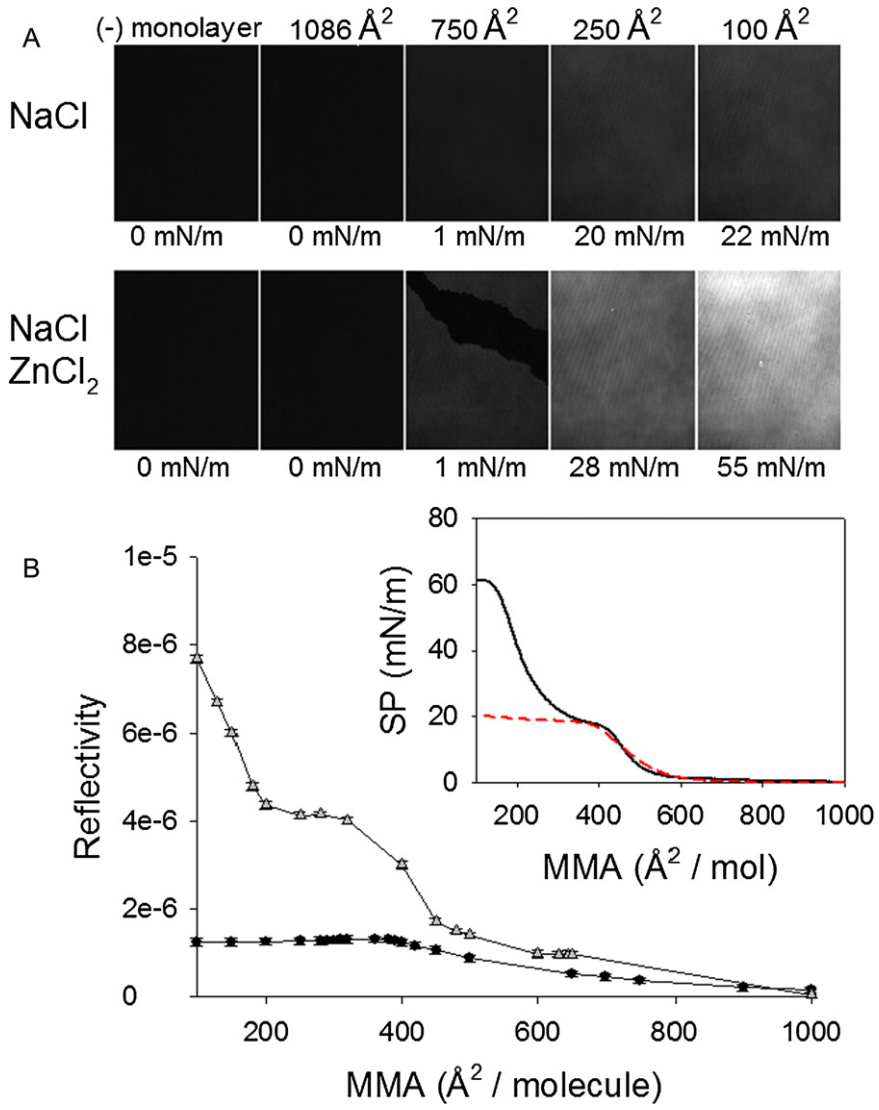

Fig. 2. Brewster angle microscopy. (A) Film topography imaged by BAM at a mean molecular area (MMA) of 1086, 750, 250 and 100 Å^2/molecule at surface pressures of 0, 1, 20 and 22 mN/m for NaCl–insulin monolayer and for $ZnCl_2$–insulin monolayer at 0, 1, 28 and 55 mN/m. Pictures were taken during compression of the films. (B) Surface reflectivity as a function of MMA. Circles and triangles correspond to NaCl–insulin monolayer and $ZnCl_2$–insulin monolayer, respectively. Inset: surface pressure (SP)–MMA isotherm of NaCl–insulin monolayer (dashed line) and $ZnCl_2$–insulin monolayer (continuous line). Average values ± SEM are result of three independent experiments.

coverslips without insulin films but in the same culture dish (and thus within the same culture medium) than the insulin-coated coverslips on which the neurons were grown. Thus, in these experiments the only source of bulk insulin in the system corresponds to that possibly desorbed from the insulin-coated monolayer. The cell density was approximately 7–9 cells per field in all conditions (Fig. 3E). By morphometric analysis we determined the polarization (axon development) stages from neurons grown onto $ZnCl_2$–insulin monolayers packed at 14 and 44 mN/m (Fig. 3F). We observed that neurons grown onto $ZnCl_2$–insulin monolayer packed at 14 mN/m polarized more than the control (58.31 ± 2.72% and 35.82 ± 5.85% stage 3 neurons, respectively) and similar to neurons stimulated by a high dose of insulin (1500 nM, Fig. 2D from supplementary material). However, polarization of neurons grown onto $ZnCl_2$–insulin monolayer packed at 44 mN/m was not different to the control (38.34 ± 1.99% and 35.93 ± 2.34% stage 3 neurons, respectively). The neurite average length was approximately 18 μm in all conditions while the axon average length was increased in neurons grown onto $ZnCl_2$–insulin monolayer packed at 14 mN/m compared to the control (115.52 ± 3.82 and 93.97 ± 4.55, respectively, Fig. 3G).

On the other hand, we cultured neurons onto (zinc-free) insulin monolayer packed at 14 mN/m (Fig. 3 supplementary material). The neuron polarization resulted in 42.29 ± 3.5% and 40.15 ± 3.6% stage 3 neurons for insulin monolayer packed at 14 mN/m and the control, respectively (Fig. 3D supplementary material). All the other measured parameters (cell density, and average length from neurites and axons) were also similar to the control. Some possibilities that may explain this fact are: (a) the surface organization of zinc-free insulin monolayer packed at 14 mN/m is not as adequate to induce neuron polarization as the $ZnCl_2$–insulin monolayer packed at 14 mN/m or, (b) the stability of the transferred monolayer may have been compromised. In order to study the latter we maintained the transferred monolayers in NaCl 145 mM at pH 7 for 22–24 h in a humidified 37 °C incubator with 5% CO_2. We measured the bulk fluorescence every hour in order to determine the insulin concentration desorbed from the monolayer. Fig. 4A shows both the absorbance and emission spectra of insulin in solution at pH 7. The emission peak of aqueous insulin was observed at 305 nm when excited at 270 nm and corresponds to the 4 tyrosine amino acids from bovine insulin [36]. The deposition of molecules onto poly L-lysine coated coverslips, by the Langmuir–Blodgett

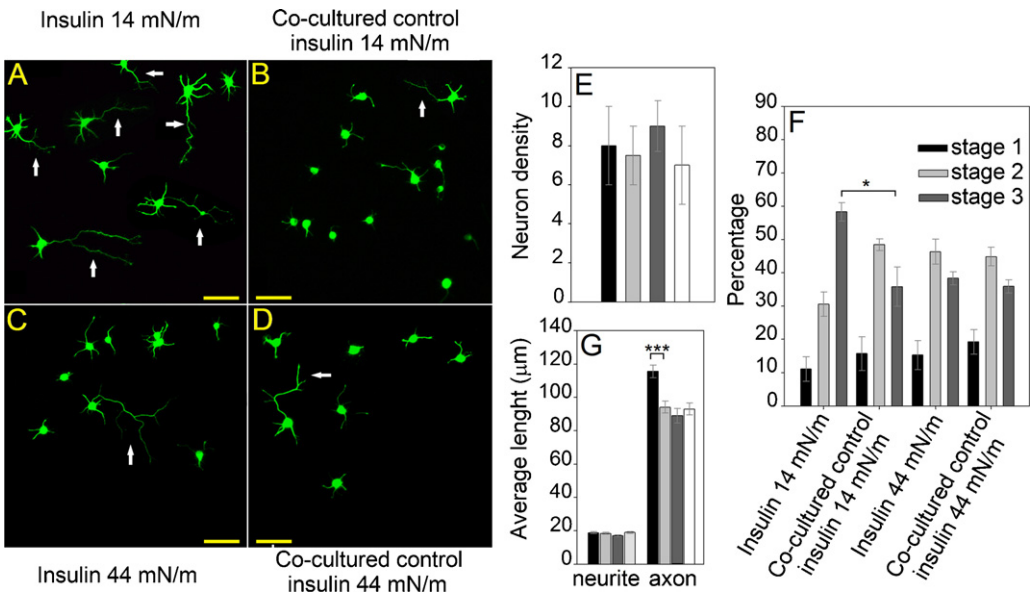

Fig. 3. Neuron polarization induced by the surface organization of $ZnCl_2$–insulin monolayers. (A) and (C) Neurons grown onto $ZnCl_2$–insulin monolayers packed at 14 mN/m and 44 mN/m, respectively. (B) and (D) Respective co-cultured controls of neurons grown onto poly L-lysine coated glasses without insulin monolayers. Arrows indicate stage 3 neurons. Neurons were immunostained with a βIII tubulin antibody. Scale bars = 50 μm. (E) neuron density per field. (F) respective percentages ± SEM of neurons at specific stages of differentiation. (G) average length of neurites and axons as a function of packing of insulin films. All data corresponds to mean ± SEM, $n = 800$ neurons from three independent experiments. ***indicates $p < 0.01$, ANOVA Bonferroni test. *indicates $p < 0.05$, Student's t test.

technique, corresponds to 5.02×10^{13} and 9.82×10^{13} molecules for monolayers transferred at 14 mN/m and 44 mN/m, respectively. If the transferred molecules were completely desorbed in the same volume that was used in the culture assays the insulin concentration derived from the coated monolayers packed at 14 mN/m and 44 mN/m would be 80 nM and 166 nM, respectively. The concentration of desorbed insulin as a function of time is shown in Fig. 4B. For the transferred $ZnCl_2$–insulin monolayer packed at 14 mN/m we observed that the desorption was 25% over the first hour and a maximal desorption, of ~50%, was reached after 3 h of incubation (Fig. 4C). A similar result was observed for the desorption of transferred $ZnCl_2$–insulin monolayer packed at 44 mN/m. By contrast, desorption of transferred zinc-free insulin monolayer packed at 14 mN/m was 6.76% after 1 h and reached 88% after 4 h. At the end of the incubation time the monolayer desorption was nearly complete. The partial desorption of $ZnCl_2$–insulin from the films explains the neuron polarization observed previously in control conditions (see Fig. 3F) where the only source of insulin comes from the fraction desorbed from the monolayer. However the bulk insulin concentration did not exceed the threshold of 100 nM where stage 3 surpass stage 2 neurons (see Fig. 2D from supplementary material). Therefore, we conclude that the differences in neuron polarization between $ZnCl_2$–insulin monolayer packed at 14 mN/m and its respective control correspond to the recognition by the neuron IGF-1 receptors of an insulin surface suitable for growth.

The release of insulin molecules from the monolayers was not a surprise. Although we observed a good transfer of monolayers to poly L-lysine coated coverslips (Fig. 1B from supplementary material) there are evidences that poly L-lysine stabilizes and also delays, but it does not abolish, the release of insulin. Encapsulated insulin in poly L-lysine-based hydrophilic star block co-polimer demonstrated substantial release at physiological pH. Moreover, the released insulin from the star block co-polymer retained its chemical integrity and immunogenicity [37]. Other authors demonstrated that the association efficiency of insulin for arginine end-functionalized derivatives of a second generation poly L-lysine dendrigraft was in the range of 99.3% to 99.7% at the relatively low molar ratio of 0.1. The released insulin retains its original conformation as revealed by circular dichroism studies [33,34]. Nevertheless, the remaining insulin on the transferred monolayer in presence of zinc ions in the subphase and packed at 14 mN/m could exert a major polarization induction compared to the other monolayers and the response of neurons grown onto this substrate appear clearly mediated by the insulin lateral organization. The axon elongation was significantly increased in neurons grown onto this monolayer (Fig. 3G). All this indicates a defined and different

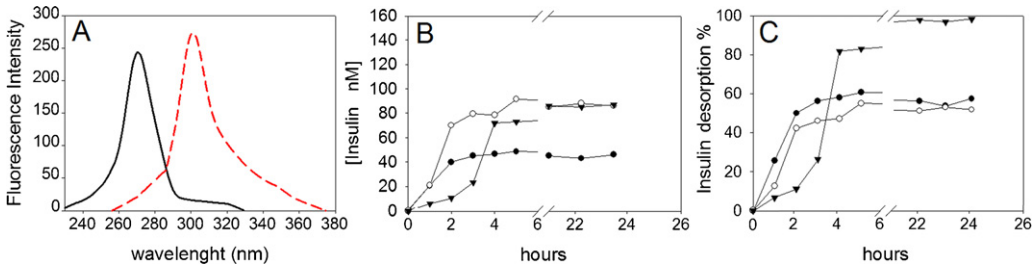

Fig. 4. Insulin monolayer stability. (A) Absorbance and fluorescence emission spectra of insulin in solution at pH 7. (B) Desorbed insulin as a function of time. (C) The same [insulin] values were converted to percentage of desorption. ●: $ZnCl_2$–insulin monolayer packed at 14 mN/m. ○: $ZnCl_2$–insulin monolayer packed at 44 mN/m. ▼: Zinc-free insulin monolayer packed at 14 mN/m.

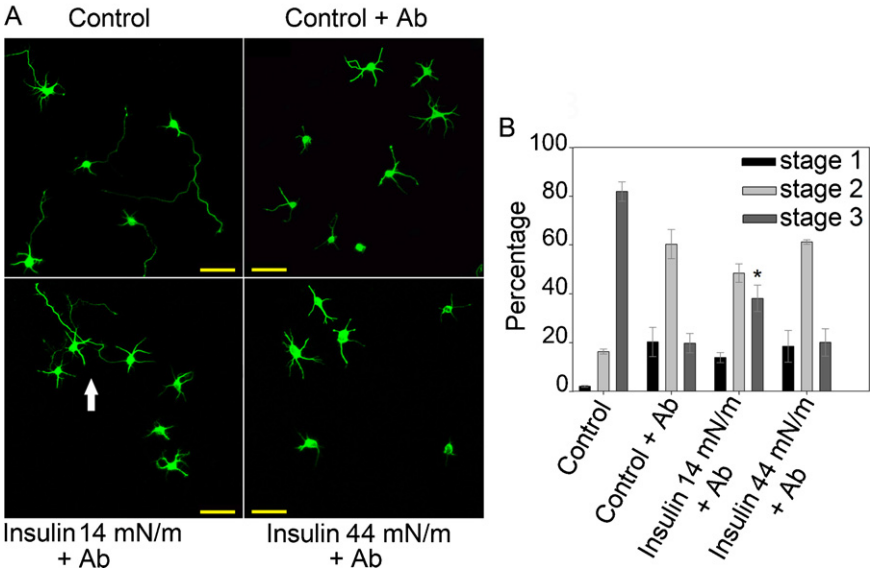

Fig. 5. IGF-1 receptor blocking. (A) Upper left panel: neurons grown onto poly L-lysine in control conditions (1500 nM insulin). *Upper right panel*: neurons grown onto poly L-lysine in control conditions plus IGF-1 receptor antibody. *Lower left and right panels*: neurons grown onto $ZnCl_2$–insulin packed at 14 and 44 mN/m, respectively, plus IGF-1 receptor antibody (arrow: neurons insensitive to the antibody). Neurons were immunostained with a β-III tubulin antibody. Scale bars = 50 μm. (B) Respective percentages ± SEM of neurons at specific stages of differentiation. All data corresponds to mean ± SEM, $n = 550$ neurons from three independent experiments. *indicates $p < 0.05$, Student's t test.

positive effect of the $ZnCl_2$–insulin monolayer packed at 14 mN/m on the neuron response, and is a direct evidence of the control of neuron polarization and axon elongation by the organization of the insulin monolayer.

In relation to this type of effects, a different cellular response to the organization of the surface for culture was also observed in Schwann cells grown onto axolemma monolayers used as culture surface; a different morphological pattern was induced when the cells are grown onto coverslips coated with axolemma packed at 34 mN/m compared to those coated with axolemma packed at 13 mN/m [19]. Those reports and the results described in the present work clearly show that the response of neural cells is selectively dependent on the different molecular organization of a same effector depending on its organization on the surface used as substrate for cell culture. This indicates that the local expression of putative surface molecules or molecular domains that may specifically mediate cell membrane recognition and triggering of signaling cascades leading to proliferative or morphogenetic cellular changes, such as neuronal polarization, are not only determined by the presence of specific external effectors but also by their long range supramolecular organization.

Related results on the effects of insulin on cell growth were observed previously. In fact, immobilized insulin stimulates the insulin receptor and signal transduction proteins for a longer period than free insulin [41]. Moreover these authors showed that immobilized fibronectin or poly L-lysine enhanced cell adhesion but not growth on porous membranes. On the other hand, immobilized insulin significantly enhanced cell growth, without affecting cell adhesion [35].

Other evidence indicates biospecific interactions. For example, antibodies against insulin inhibit the cell proliferation induced by immobilized insulin [38]. In addition, immobilized insulin accelerates the growth of anchorage-dependent cells, but does not accelerate that of anchorage-independent cells such as hybridomas [39,40]. These findings suggest that adhesion, or the interaction of cells with the substrate immobilized with insulin, is necessary for growth stimulation [35]. Thus, as suggested above, $ZnCl_2$–insulin organized as a monolayer packed at 14 mN/m induces not only polarization but also neuron growth through IGF-1 receptor activation, as shown in Fig. 3G. This possibility was confirmed at a molecular level by blocking the IGF-1 receptor as described in the next section.

3.3. Blocking of the IGF-1 receptor

An early event in axonal specification during neuronal differentiation is the enrichment of IGF-1 receptors in one minor neurite at stage 2 of differentiation [5]. To be activated, the IGF-1 receptor needs to be inserted into the neuronal membrane so that the ligand binding site is exposed to the extracellular space. Therefore, we studied the consequences of loss of function of IGF-1 receptor by using a specific antibody as described previously [5]. Fig. 5 shows the IGF-1 receptor blocking experiment. As seen in the figure, addition of the IGF-1 receptor blocking antibody to the culture medium prevented polarization in control condition (bulk insulin 1500 nM) so most neurons remained at stage 2 of differentiation (60.08 ± 6.0%). The stage 3 neurons decreased to 19.7 ± 4.0%. A similar result was observed in neurons grown onto $ZnCl_2$–insulin monolayer packed at 44 mN/m (61.0 ± 0.91% and 20.0 ± 5.62% neurons in stage 2 and 3, respectively). However, even if we observed a decrease of neuronal polarization in $ZnCl_2$–insulin packed at 14 mN/m, the loss of function of IGF-1 receptor was significantly lower than in the control condition (38.0 ± 5.33% vs. 19.7 ± 4.0% neurons in stage 3, respectively). As negative control the IGF-1 receptor antibody was not added to the medium with 1500 nM insulin and the polarization reached 81.75 ± 4.0%.

It was shown previously that IGF-1 and its receptor, which regulate exocytosis of plasmalemmal precursor vesicles (PPVs) at the axonal growth cone, are essential for the establishment of neuronal polarity [5]. IGF-1 could exert its influence on axon specification via a number of different mechanisms including pathways that do not include membrane expansion. However, activation of the IGF-1 receptor requires its insertion into the plasmalemma. By probing for the appearance of activated IGF-1 receptor in undifferentiated neurites, Dupraz et al. [8] demonstrated that the exocyst complex (PPVs) is necessary for IGF-1 receptor externalization in non-polarized neurons. Thus, insertion of IGF-1 receptor in an undifferentiated neurite is necessary for polarization. The blocking

experiment demonstrated that IGF-1 receptor was present and activatable in neurites from neurons in stage 2. It was well apparent under control conditions and in neurons grown onto $ZnCl_2$–insulin packed at 44 mN/m. However, the relative lack of blocking efficiency of IGF-1receptor antibody seen in neurons grown onto $ZnCl_2$–insulin packed at 14 mN/m was intriguing. Mainly two possibilities may account for this phenomenon: on one hand, the lateral diffusion of IGF-1 receptor antibody could be impaired under the attached membrane surface of the neurons, where the local insulin concentration in the transferred monolayers might be locally higher and binding more efficient at 14 mN/m; on the other hand, the binding equilibrium of IGF-1 receptor itself could be more favorably displaced toward insulin rather than to the antibody against IGF-1 receptor. Further experiments are needed to explore these possibilities in order to better understand the effect on molecular terms.

3.4. Growth cone morphology and attachment observed by surface reflection interference contrast (SRIC)

After incubation of neurons in control condition, or grown onto $ZnCl_2$–insulin monolayers packed at 14 mN/m or 44 mN/m, the cultures were fixed and analyzed using a Nikon Eclipse TIRF microscope with SRIC capability. SRIC microscopy is based on interference of waves coming from different interphases and it makes visible, in black, the cell structures in close contact with the surface. Fig. 6 shows phase contrast images of neurons and SRIC images of growth cones: a and b corresponds to growth cones of a neuron in stage 2 and 3, respectively under control conditions (high insulin concentration). As seen in the figure, the pattern of attachment regions in the growth cones appears black. A similar result was observed in stage 2 neurons (Fig. 6c) grown onto $ZnCl_2$–insulin monolayer packed at 14 mN/m. Interestingly,

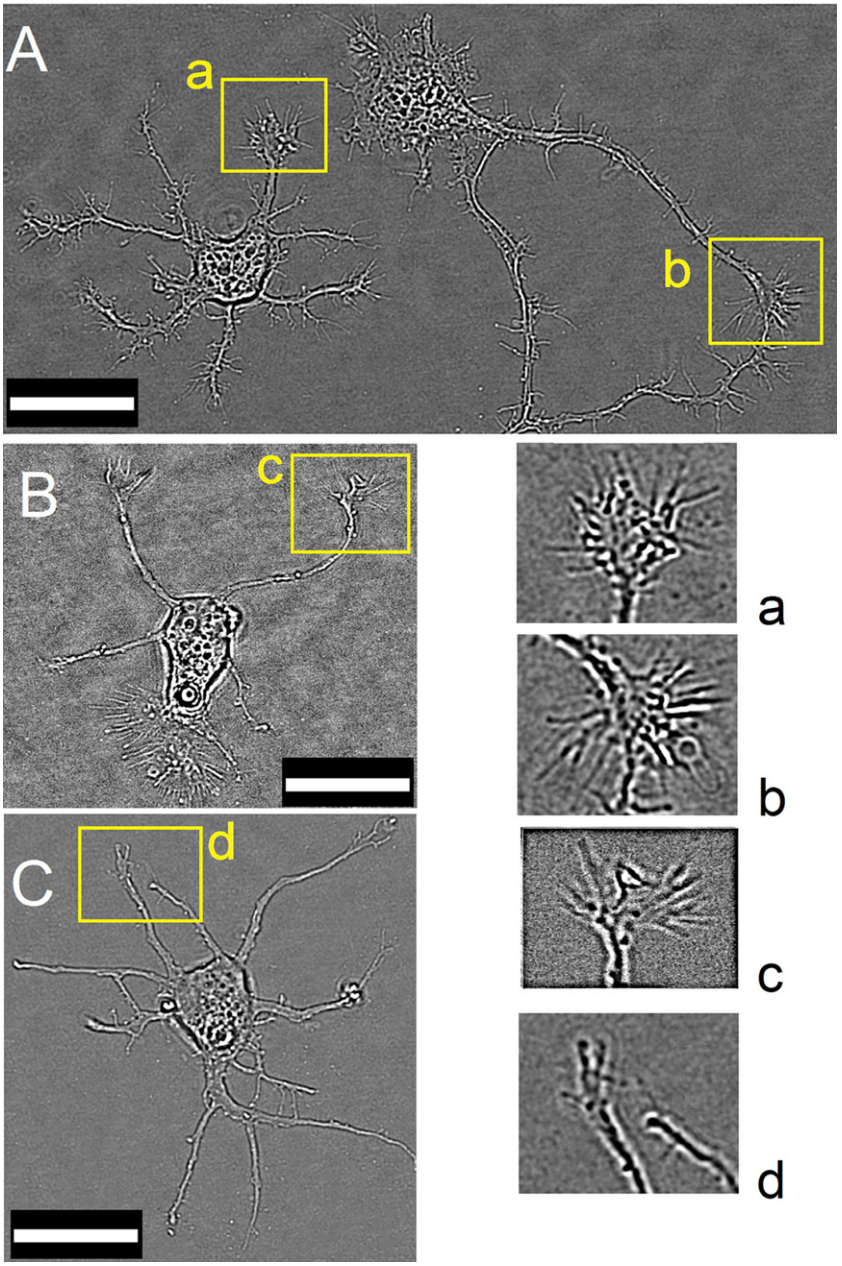

Fig. 6. Phase contrast and SRIC of neurons. A, B, C: phase contrast of control neurons (A) and neurons grown onto insulin monolayer packed at 14 mN/m (B) and 44 mN/m (C). a, b, c, d: SRIC images of growth cones (2× digital magnification from original phase contrast images, square boxes in A, B, C). Scale bars = 20 μm.

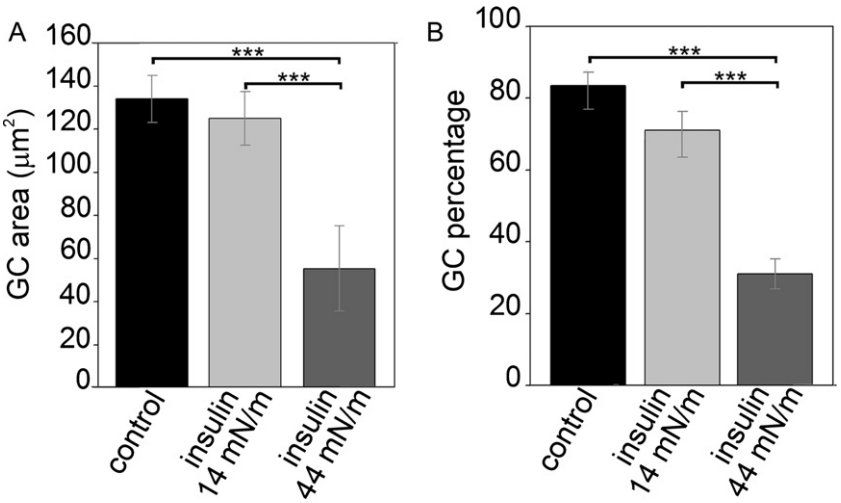

Fig. 7. Morphological analyses of expanded growth cones. (A) Average area (μm^2 of expanded growth cones (GC) shown in Fig. 6 (a, b, c, d). (B) Percentage of neurons that have at least one expanded cone (GC) with an area of at least 30 μm^2. All data corresponds to mean ± SEM, $n = 250$ neurons from three independent experiments. ***corresponds to $p < 0.05$, ANOVA Bonferroni-test.

neurons grown onto $ZnCl_2$–insulin monolayer packed at 44 mN/m showed lower growth cone development (Fig. 7). The mean growth cone area was 133.94 ± 10.88 μm^2 for control neurons (high insulin in bulk), 125.01 ± 12.48 μm^2 and 55.26 ± 19.73 μm^2 for neurons grown onto $ZnCl_2$–insulin monolayers packed at 14 and 44 mN/m, respectively (Fig. 7A). By calculating the statistical mode on the total population of measured neurons, an area of 30 μm^2 can be taken as threshold for the definition of an expanded growth cone. Fig. 7B shows the percentage of neurons that have at least one expanded growth cone. We observed that growth cone expansion was dependent on both the insulin availability and its surface organization. The higher percentage was observed for control with high insulin concentration in bulk (82.2 ± 5.2%), followed by neurons grown onto $ZnCl_2$–insulin monolayers packed at 14 mN/m (71.1 ± 7.5%). The lower growth cone expansion was observed in neurons grown onto $ZnCl_2$–insulin monolayer packed at 44 mN/m (31.3 ± 4.2%). Note that the percentage of neurons bearing at least one expanded growth cone shows a striking correlation with the

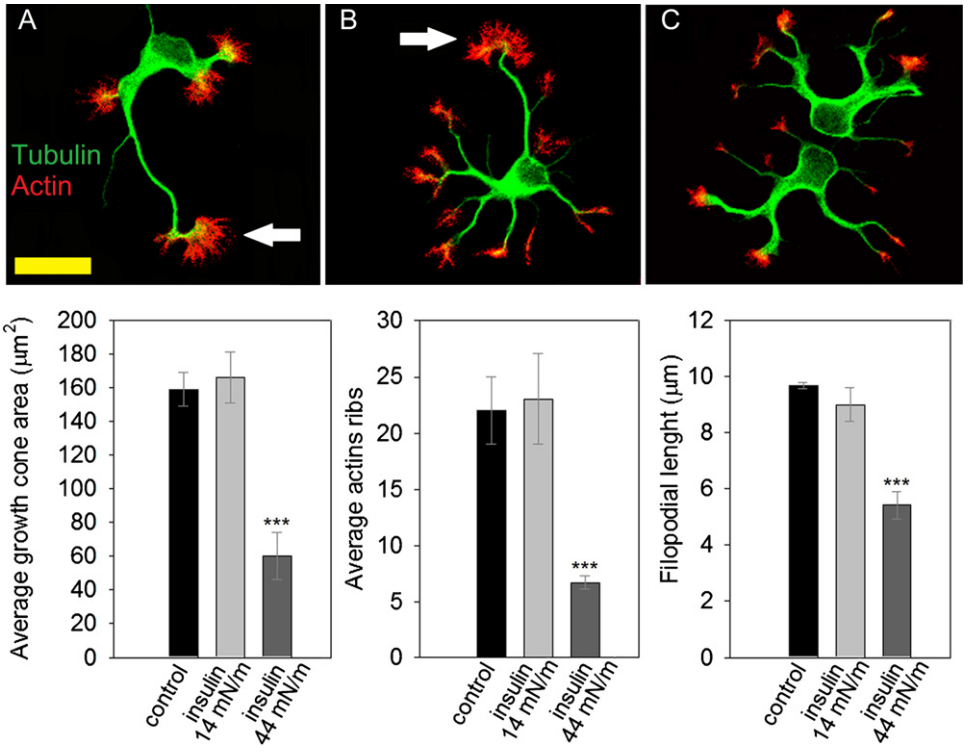

Fig. 8. The morphology and cytoskeletal organization of growth cones. *Upper panels*: red–green overlays of growth cones showing the distribution of β-III microtubules (green) and F-actin (red) in control neurons (A) and neurons grown onto $ZnCl_2$–insulin monolayers packed at 14 and 44 mN/m (B and C, respectively). In control neurons (A) and in neurons grown onto $ZnCl_2$–insulin monolayers packed at 14 mN/m (B), a central microtubule-containing zone is completely surrounded by a radially oriented array of F-actin (arrows). *Lower panels*: quantification of growth cone shape parameters in neurons with 1500 insulin in bulk (control) and neurons grown onto $ZnCl_2$–insulin monolayers packed at 14 and 44 mN/m as indicated in the figure. ***means $p < 0.01$, ANOVA Bonferroni test. (For interpretation of the references to color in this figure legend, the reader is referred to the web version of the article.)

amount of cells which exhibited a polarized morphology in the different conditions assayed (see above Fig. 3). This interesting correlation may be explained in terms of IGF-1 receptor activation by optimal surface organization of insulin.

These results were corroborated by confocal microcospy observing growth cones of neurons double stained with antibodies against β-III tubulin and rhodamine-phalloidin for F-actin. The immunostaining revealed a central microtubule-containing zones completely surrounded by a radially orientated array of F-actin [42], from which numerous and short filipodial extensions emerge (Fig. 8). There were no significant alterations in growth cone morphology, size, filopodial number, and/or the pattern of distribution of microtubules and actin filaments between neurons cultured in control condition (1500 nM insulin) and neurons grown onto $ZnCl_2$–insulin monolayers packed at 14 mN/m (Fig. 8A and B). By contrast, when neurons were cultured onto $ZnCl_2$–insulin monolayers packed at 44 mN/m, a significant change of growth cone shape was induced (Fig. 8C). These alterations involved a dramatic reduction of growth cone area, disappearance of radial striations and a reduction in the number of filopodia (Fig. 8, lower pannels).

4. Conclusions

It is widely known that neuron polarization is triggered by external cues such as IGF-1 or insulin, among others. However, it is less clear whether these molecules can exert different cellular effects in terms of their molecular organization. In this work we demonstrate that insulin organized as a monomolecular film is capable of finely regulating neuron polarization and morphological response of guiding axon growth cones depending on changes of the insulin molecular organization of the film used as growth surface. These findings reveal the existence of sensitive transducing mechanisms involving the neuron membrane that extend to internal structures and selectively respond to supramolecular signals from the film surface that can go beyond molecular specificity in their regulation of cellular function.

Acknowledgements

This work was supported by grants from SECYT-UNC, FONCyT and CONICET, Argentina. Confocal microscopy analyses were performed in the Microscopy Laboratory (affiliated to Sistema Nacional de Microscopía, MINCyT, Argentina) located in CIQUIBIC UNC, Córdoba, Argentina.

Appendix A. Supplementary data

Supplementary data associated with this article can be found, in the online version, at doi:10.1016/j.colsurfb.2013.01.059.

References

[1] F. Bradke, C.G. Dotti, Science 283 (1999) 1931.
[2] H. Bito, T. Furuyashiki, H. Ishihara, Y. Shibasaki, K. Ohashi, K. Mizuno, M. Maekawa, T. Ishizaki, S. Narumiya, Neuron 26 (2000) 431.
[3] P. Kunda, G. Paglini, S. Quiroga, K. Kosik, A. Cáceres, J. Neurosci. 21 (2001) 2361.
[4] B.K. Garvalov, K.C. Flynn, D. Neukirchen, L. Meyn, N. Teusch, X. Wu, C. Brakebusch, J.R. Bamburg, F. Bradke, J. Neurosci. 27 (2007) 13117.
[5] L. Sosa, S. Dupraz, L. Laurino, F. Bollati, M. Bisbal, A.A. Cáceres, K.H. Pfenninger, S. Quiroga, Nat. Neurosci. 9 (2006) 993.
[6] S. Quiroga, R.S. Garofalo, K.H. Pfenninger, Proc. Natl. Acad. Sci. U.S.A. 92 (1995) 4309.
[7] T. Nishimura, Y. Fukata, K. Kato, T. Yamaguchi, Y. Matsuura, H. Kamiguchi, K. Kaibuchi, Nat. Cell Biol. 5 (2003) 819.
[8] S. Dupraz, D. Grassi, M.E. Bernis, L. Sosa, M. Bisbal, L. Gastaldi, I. Jausoro, A. Cáceres, K.H. Pfenninger, S. Quiroga, J. Neurosci. 42 (2009) 13292.
[9] K.H. Pfenninger, M.F. Maylié-Pfenninger, J. Cell Biol. 89 (1981) 536.
[10] K.H. Pfenninger, L.B. Friedman, Brain Res. Dev. Brain Res. 71 (1993) 181.
[11] A.H. Futerman, G.A. Banker, Trends Neurosci. 19 (1996) 144.
[12] K.H. Pfenninger, L. Laurino, D. Peretti, X. Wang, S. Rosso, G. Morfini, A. Cáceres, S. Quiroga, J. Cell Sci. 116 (2003) 1209.
[13] L. Laurino, X.X. Wang, B.A. de la Houssaye, L. Sosa, S. Dupraz, A. Cáceres, K.H. Pfenninger, S. Quiroga, J. Cell Sci. 118 (2005) 3653.
[14] K.H. Pfenninger, Nat. Rev. Neurosci. 10 (4) (2009) 251–261.
[15] H.M. McConnell, T.H. Watts, R.M. Weiss, A.A. Brian, Biochim. Biophys. Acta 864 (1986) 95.
[16] A. Kloboucek, A. Behrisch, J. Faix, E. Sackmann, Biophys. J. 77 (1999) 2311.
[17] C.C. Blackburn, P. Swank-Hill, R.L. Schnaar, J. Biol. Chem. 261 (1986) 2873.
[18] H. Rösner, Ann. N.Y. Acad. Sci. 845 (1998) 200.
[19] R.O. Calderón, B. Maggio, T.J. Neuberger, G.H. De Vries, J. Neurosci. Res. 34 (1993) 206.
[20] R.O. Calderón, B. Maggio, T.J. Neuberger, G.H. DeVries, J. Neurosci. Res. 40 (1995) 349.
[21] T. Esch, V. Lemmon, G. Banker, J. Neurosci. 19 (1999) 6417.
[22] T. Yoshimura, N. Arimura, K. Kaibuchi, Ann. N.Y. Acad. Sci. 1086 (2006) 116.
[23] C. Ménager, N. Arimura, Y. Fukata, K. Kaibuchi, J. Neurochem. 89 (2004) 109.
[24] M. Nieto-Suárez, N. Vila-Romeu, I. Prieto, Thin Solid Films 516 (2008) 8873.
[25] S. Pérez-López, N.M. Blanco-Vila, N. Vila-Romeu, J. Phys. Chem. B 115 (2011) 9387.
[26] W. Liu, S. Johnson, M. Micic, J. Orbulescu, J. Whyte, A.R. Garcia, R.M. Leblanc, Langmuir 28 (2012) 3369.
[27] H. Brockman, Chem. Phys. Lipids 3 (1994) 57.
[28] G.L.J. Gaines, Insoluble Monolayers at Liquid−Gas Interfaces, Wiley-Interscience, New York, 1966, p. 136.
[29] C.M. Rosetti, B. Maggio, R.G. Oliveira, Biochim. Biophys. Acta 1778 (2008) 1665.
[30] S. Rosso, F. Bollati, M. Bisbal, D. Peretti, T. Sumi, T. Nakamura, S. Quiroga, A. Ferreira, A. Cáceres, Mol. Biol. Cell 15 (2004) 3433.
[31] S. Johnson, W. Liu, G. Thakur, A. Dadlani, R. Patel, J. Orbulescu, J.D. Whyte, M. Micic, R.M. Leblanc, J. Phys. Chem. B (2012) (Epub ahead of print).
[32] M.J. Adams, T.L. Blundell, E.J. Dodson, G.G. Dodson, M.E. Vijavayan, N. Baker, M.M. Harding, D.C. Hodgkin, B. Rimmer, S. Sheat, et al., Nature 224 (1969) 491.
[33] M. Bouchard, J. Zurdo, E.J. Nettleton, C.M. Dobson, C.V. Robinson, Protein Sci. 9 (2000) 1960.
[34] Z. Sideratou, N. Sterioti, D. Tsiourvas, L.A. Tziveleka, A. Thanassoulas, G. Nounesis, C.M. Paleos, J. Colloid Interface Sci. 351 (2010) 433.
[35] Y. Ito, J. Zheng, Y. Imanishi, Biomaterials 18 (1997) 197.
[36] N.C. Santos, M. Castanho, Trends Appl. Spectrosc. 4 (2002) 113.
[37] Y. Yan, D. Wei, J. Li, J. Zheng, G. Shi, W. Luo, Y. Pan, J. Wang, L. Zhang, X. He, D. Liu, Acta Biomater. 8 (2012) 2113.
[38] S.Q. Liu, Y. Ito, Y. Imanishi, Biomaterials 13 (1992) 50.
[39] J. Zheng, Y. Ito, Y. Imanishi, Biotechnol. Prog. 11 (1995) 677.
[40] Y. Ito, T. Uno, S.Q. Liu, Y. Imanishi, Biotechnol. Bioeng. 40 (1992) 1271.
[41] Y. Ito, J. Zheng, Y. Imanishi, K. Yonezawa, M. Kasuga, Proc. Natl. Acad. Sci. U.S.A. 93 (1996) 3598.
[42] G. Paglini, P. Kunda, S. Quiroga, K. Kosik, A. Cáceres, J. Cell Biol. 143 (1998) 443.